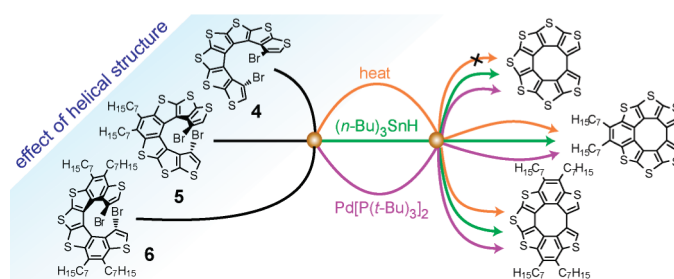


Intramolecular Cyclization of Thiophene-Based [7]Helicenes to Quasi-[8]Circulenes

Andrzej Rajca,^{*,†} Makoto Miyasaka,[†] Shuzhang Xiao,[†] Przemysław J. Boratyński,^{†,§} Maren Pink,[‡] and Suchada Rajca[†][†]Department of Chemistry, University of Nebraska, Lincoln, Nebraska 68588-0304, and [‡]IUMSC, Department of Chemistry, Indiana University, Bloomington, Indiana 47405-7102. [§]On leave from Politechnika Wrocławska, Poland.

arajca1@unl.edu

Received September 21, 2009



Intramolecular cyclization in a series of thiophene-based dibromof[7]helicenes (**4–6**) with different helix structures is investigated by vacuum pyrolysis, tin- and palladium-mediated C–C bond forming reactions. The product with the cyclic structure of the annelated aromatic rings, which resembles [8]circulene devoid of an atom linkage, is referred to as quasi-[8]circulene. Vacuum pyrolysis of **4** gives insoluble, unidentified products, while **5** and **6** yield the corresponding quasi-[8]circulenes under similar conditions. Thermogravimetry (TG) and differential scanning calorimetry (DSC) analyses for **4** indicate complex reaction pathways, while those for **5** and **6** show a single process corresponding to a loss of 1 equiv of Br₂ at about 330 °C. Pd-mediated reductive cyclization provides quasi-[8]circulenes for all three [7]helicenes, though only **4** gives a good isolated yield. Tributyltin hydride-mediated radical cyclization of **4–6** provides quasi-[8]circulenes in excellent yields, and it is practically insensitive to the helix structure. Experimental and calculated UV–vis absorption spectra for quasi-[8]circulenes and [8]circulenes are reported. The results suggest that the lack of atom linkage in quasi-[8]circulene does not significantly affect properties and conformation, compared to those for the corresponding [8]circulenes.

Introduction

Oligomers of [*n*]helicenes that are connected through C–C bonds at their inner rims are predicted to provide rigid helices with extraordinary preference for helical folding.¹ For example, carbon–sulfur bis[7]helicene **1**, in which the two [7]helicene moieties have the same configuration, adopts rigid, helically locked conformation both in the solid state and in solution (Figure 1).¹

The convergent synthetic route to “helically-locked” oligomers of [*n*]helicenes could rely on intermolecular C–C bond homocoupling reactions of functionalized [*n*]helicenes with adequate solubility. However, we find that such an approach

is hindered by the competing intramolecular cyclization, as illustrated by the C–C bond formation at the inner helical termini of dibromof[7]helicene **2** to product **3** (Scheme 1).

The cyclic structure of the annelated aromatic rings such as **3** is an intriguing oligothiophene with a planar, cross-conjugated π-system,^{2,3} and it appears to resemble the Nenajdenko’s “sulflower”, carbon–sulfur [8]circulene (C₂S)₈,^{4–6} a

(2) Mishra, A.; Ma, C.-Q.; Bäuerle, P. *Chem. Rev.* **2009**, *109*, 1141–1276.(3) (a) Gholami, M.; Tykwinski, R. R. *Chem. Rev.* **2006**, *106*, 4997–5027.(b) Nielsen, M. B.; Diederich, F. *Chem. Rev.* **2005**, *105*, 1837–1868.(4) Chernichenko, K. Y.; Sumerin, V. V.; Shpanchenko, R. V.; Balenkova, E. S.; Nenajdenko, V. G. *Angew. Chem., Int. Ed.* **2006**, *45*, 7367–7370.(5) Chernichenko, K. Y.; Balenkova, E. S.; Nenajdenko, V. G. *Mendeleev Commun.* **2008**, *18*, 171–179.(6) Bukalov, S. S.; Leites, L. A.; Lyssenko, K. A.; Aysin, R. R.; Korlyukov, A. A.; Zubavichus, J. V.; Chernichenko, K. Y.; Balenkova, E. S.; Nenajdenko, V. G.; Antipin, M. Y. *J. Phys. Chem. A* **2008**, *112*, 10949–10961.(1) Miyasaka, M.; Pink, M.; Rajca, S.; Rajca, A. *Angew. Chem., Int. Ed.* **2009**, *48*, 5954–5957.

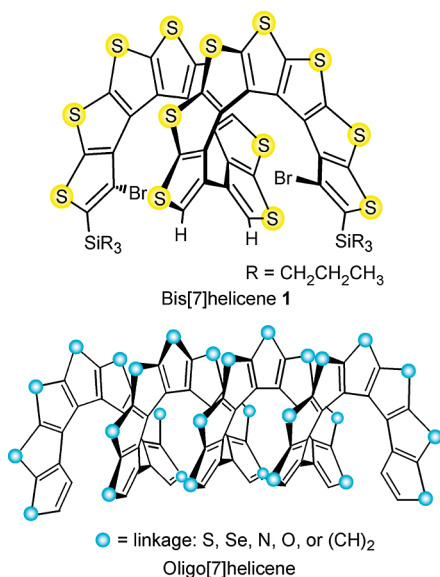
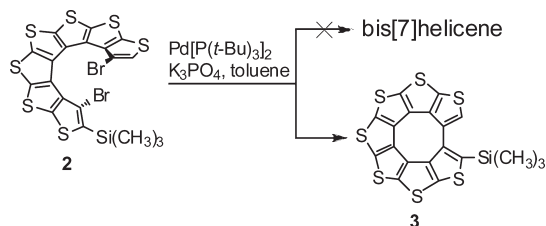


FIGURE 1. Bis[7]helicene and oligo[7]helicene.

SCHEME 1



beautiful molecule with potentially important materials properties but with very limited solubility (Figure 2).^{7,8} We note that the α -CH positions of thiophenes in **3** would enable functionalization, which is not possible in the carbon–sulfur [8]circulene, thus providing an avenue to the cyclic structure of annelated aromatic rings with improved solubility and/or as building blocks for extended macromolecular structures and assemblies.

Other conjugated cyclic structures similar to **3** are known in the synthetic pathways to [n]circulenes. In Yamamoto's photosynthesis of [7]circulene, the Reiss' "hexa[7]circulenes" were used as key synthetic precursors.^{9,10} Wynberg and co-workers reported synthesis of heterocirculenes from "dehydrohelicenes", compounds in which the two termini of a

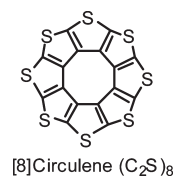


FIGURE 2. Carbon–sulfur [8]circulene (C₂S)₈.

helicene are connected by a σ bond, formed by dehydrogenation of [5]helicenes and [6]helicenes, using a Scholl-type reaction.¹¹ Notably, all these examples are limited to the cyclic structures of 5 and 6 annelated aromatic rings devoid of solubilizing groups, and thus they possess exceedingly low solubility. As it appears, the nomenclature for these conjugated cyclic structures is not established, we refer to **3** as carbon–sulfur quasi-[8]circulene.¹²

In addition to the appeal as direct precursors to [n]circulenes and building blocks for extended structures and assemblies, the structure of these quasi-[n]circulenes poses an interesting question, whether the lack of an atom linkage would significantly affect electronic structure and conformation, compared to those for the corresponding [n]circulenes. For comparison, chiroptical properties of bis[7]helicene **1** are similar to those calculated for the corresponding [15]helicene, suggesting that the absence of sulfur linkage in **1** has only a minor effect on the chiroptical properties and on the conformation, compared to the [15]helicene.¹

We have recently prepared a series of dibromo[7]helicenes (**4–6**) and their trimethylsilyl derivatives, both as racemic and enantiomerically pure products, and obtained their X-ray single crystal structures.^{13–16} Thus, we have an avenue to examine intramolecular cyclization of dibromo[7]helicenes to quasi-[8]circulenes. The helix structure of [7]helicenes **4–6** dictates the proximity of the two helical termini and the relative orientation of the C–Br bonds. Therefore, the C–C bond formation at the two helical termini of the [7]helicenes may presumably be more efficient when the C \cdots C distance (r) is shorter or the Br–C–C–Br torsion angle (ϕ) is approximately within the coplanar arrangement ($\phi \approx 180^\circ$). We note that the average ϕ values determined from the X-ray structures of **4**, **5**, and **6** are 176° , 153° , and 146° , respectively; in the same series, the C \cdots C distances decrease from about 4 Å to 3.3 Å (Figure 3).¹⁷

We consider vacuum pyrolysis, tin- and palladium-mediated C–C bond forming reactions. There are a plethora of precedents for cyclization of bromoaryls and dibromoaryls, forming C–C bonds, using flash vacuum pyrolysis and

(7) Material properties of (C₂S)₈: (a) Dadvand, A.; Cicoira, F.; Chernichenko, K. Y.; Balenkova, E. S.; Osuna, R. M.; Rosei, F.; Nenajdenko, V. G.; Perepichka, D. F. *Chem. Commun.* **2008**, 5354–5356. (b) Gahungu, G.; Zhang, J.; Barancira, T. *J. Phys. Chem. A* **2009**, *113*, 255–262. (c) Ivasenko, O.; MacLeod, J. M.; Chernichenko, K. Y.; Balenkova, E. S.; Shpanchenko, R. V.; Nenajdenko, V. G.; Rosei, F.; Perepichka, D. F. *Chem. Commun.* **2009**, 1192–1194. (d) Gahungu, G.; Zhang, J. *J. Phys. Chem. Chem. Phys.* **2008**, *10*, 1743–1747. (e) Fujimoto, T.; Suizu, R.; Yoshikawa, H.; Awaga, K. *Chem.—Eur. J.* **2008**, *14*, 6053–6056. (f) Fujimoto, T.; Matsushita, M. M.; Awaga, K. *J. Am. Chem. Soc.* **2008**, *130*, 15790–15791.

(8) [8]Circulenes with alternating benzene and furan rings: (a) Eskildsen, J.; Reenberg, T.; Christensen, J. B. *Eur. J. Org. Chem.* **2000**, 1637–1640. (b) Erdtman, H.; Högberg, H.-E. *Tetrahedron Lett.* **1970**, *38*, 3389–3392. (c) Högberg, H.-E. *Acta Chem. Scand.* **1972**, *26*, 2752–2758.

(9) Jessup, P. J.; Reiss, J. A. *Tetrahedron Lett.* **1975**, 1453–1456.

(10) (a) Yamamoto, K.; Harada, T.; Okamoto, Y.; Chikamatsu, H.; Nakazaki, M.; Kai, Y.; Nakao, T.; Tanaka, M.; Harada, S.; Kasai, N. *J. Am. Chem. Soc.* **1988**, *110*, 3578–3584. (b) Yamamoto, K. *Pure Appl. Chem.* **1993**, *65*, 157–163. (c) Sato, M.; Yamamoto, K.; Sonobe, H.; Yano, K. *J. Chem. Soc., Perkin 2* **1998**, 1909–1913.

(11) (a) Dopfer, J. H.; Oudman, D.; Wynberg, H. *J. Org. Chem.* **1975**, *40*, 3398–3401. (b) Dopfer, J. H.; Wynberg, H. *J. Org. Chem.* **1975**, *40*, 1957–1966.

(12) [m]Circulene is commonly defined as a circulene constructed out of *m* aromatic rings. Quasi is a prefix meaning "resembling" or "in some manner" and it is usually hyphenated to a noun. Therefore, we propose to refer to cyclic compounds analogous to [m]circulenes, but composed of only *m* – 1 aromatic rings, as quasi-[m]circulenes.

(13) Rajca, A.; Miyasaka, M.; Pink, M.; Wang, H.; Rajca, S. *J. Am. Chem. Soc.* **2004**, *126*, 15211–15222.

(14) Miyasaka, M.; Rajca, A.; Pink, M.; Rajca, S. *Chem.—Eur. J.* **2004**, *10*, 6531–6539.

(15) Rajca, A.; Pink, M.; Xiao, S.; Miyasaka, M.; Rajca, S.; Das, K.; Plessel, K. *J. Org. Chem.* **2009**, *74*, 7504–7513.

(16) Rajca, A.; Wang, H.; Pink, M.; Rajca, S. *Angew. Chem., Int. Ed.* **2000**, *39*, 4481–4483.

(17) The X-ray crystallographically determined helical shapes are similar to those calculated at the B3LYP/6-31G(d,p) level of theory (Table S1, S1).

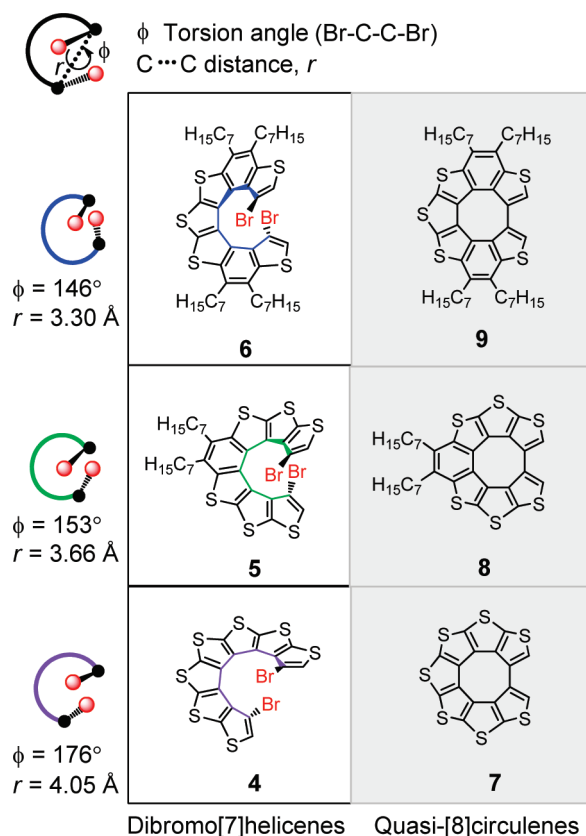


FIGURE 3. Dibromo[7]helicenes and the corresponding quasi-[8]circulenes.

vacuum pyrolysis to provide both planar and curved polycyclic aromatic compounds.^{18–21} Tin- and palladium-mediated cyclization of dibromo[7]helicenes 4–6 could provide an advantage of much lower reaction temperatures than vacuum pyrolysis.²² In particular, the bis(*tri-tert*-butylphosphine)palladium/ K_3PO_4 catalytic system²³ was shown to be effective for typically difficult C–C bond formation between the β -positions of the sterically hindered bromo-thiophene derivatives.^{24–26}

Here we report the intramolecular cyclization in a series of [7]helicenes, for which we optimize the cyclization reactions in 4–6 to provide a synthetic pathway to quasi-[8]circulenes 7–9 (Figure 3).

(18) Scott, L. T.; Boorum, M. M.; McMahon, B. J.; Hagen, S.; Mack, J.; Blank, J.; Wegner, H.; de Meijere, A. *Science* **2002**, *295*, 1500–1503.

(19) Marcinow, Z.; Grove, D. I.; Rabideau, P. W. *J. Org. Chem.* **2002**, *67*, 3537–3539.

(20) Amick, A. W.; Wakamiya, A.; Scott, L. T. *J. Org. Chem.* **2008**, *73*, 5119–5122.

(21) For review, see: Tsefrikas, V. M.; Scott, L. T. *Chem. Rev.* **2006**, *106*, 4868–4884.

(22) For recent examples of tin-mediated radical cyclizations forming aryl–aryl C–C bonds, see: (a) Radix, S.; Barret, R. *Tetrahedron* **2007**, *63*, 12379–12387. (b) Takeuchi, K.; Ishita, A.; Matsuo, J.; Ishibashi, H. *Tetrahedron* **2007**, *63*, 11101–11107. (c) Harrowven, D. C.; Guy, I. L.; Nanson, L. *Angew. Chem., Int. Ed.* **2006**, *45*, 2242–2245. (d) Wang, Y.-C.; Lin, C.-H.; Chen, C.-M.; Liou, J.-P. *Tetrahedron Lett.* **2005**, *46*, 8103–8104.

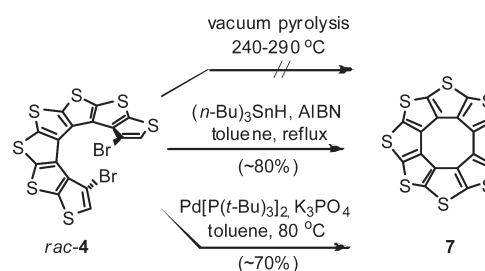
(23) Dai, C.; Fu, G. C. *J. Am. Chem. Soc.* **2001**, *123*, 2719–2724.

(24) Miyasaka, M.; Rajca, A. *Synlett* **2004**, 177–182.

(25) Miyasaka, M.; Rajca, A.; Pink, M.; Rajca, S. *J. Am. Chem. Soc.* **2005**, *127*, 13806–13807.

(26) Rajca, A.; Rajca, S.; Pink, M.; Miyasaka, M. *Synlett* **2007**, 1799–1822.

SCHEME 2. Carbon–Sulfur Quasi-[8]Circulene 7



Results and Discussion

Quasi-[8]circulene 7. When dibromo[7]helicene *rac-4* is heated to $\sim 240^\circ\text{C}$ under vacuum in a sealed capillary, the color of the sample gradually darkens without melting, and after several hours at $\sim 240^\circ\text{C}$ a black solid is obtained. The solid is only partially soluble in organic solvents. In chloroform-*d*, the ^1H NMR spectrum shows a weak singlet at the chemical shift corresponding to the starting material *rac-4*, with no evidence for quasi-[8]circulene 7 (Scheme 2). A significant increase in the temperature of pyrolysis (50°C) leads to complete conversion of starting material *rac-4*, to give a black, insoluble solid for which high-field ^1H NMR spectra in organic solvents such as chloroform-*d* or benzene-*d*₆ could not be obtained even with the aid of a cryoprobe.

Pyrolysis of dibromo[7]helicene *rac-4* was monitored by simultaneous thermogravimetry (TG) and differential scanning calorimetry (DSC). The DSC plot shows no intense peaks, and three processes associated with mass loss at 200, 270, and 400°C are observed in the TG plot (Figure S12, SI), suggesting complex reaction pathways.²⁷

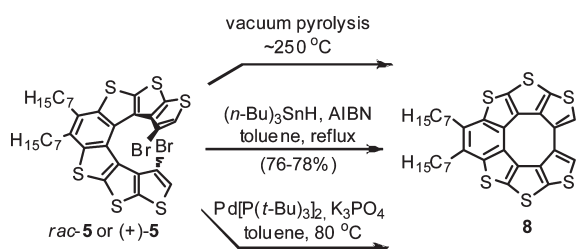
Tributyltin hydride-mediated radical cyclization of *rac-4* provides a relatively clean crude reaction mixture, as indicated by ^1H NMR spectra (Figures S18 and S21, SI); upon washing with methanol and acetone, a poorly soluble colorless quasi-[8]circulene 7 is obtained in 80% yield. The solubility of 7 is markedly decreased after purification to the extent that the signature singlet ^1H -resonance at δ 7.95 ppm for 7 is difficult to detect even with the aid of a cryoprobe. The mass spectrum (EI) of 7 shows the peak corresponding to M^+ that has dominant intensity in the m/z 150–440 range and exact mass of 417.8204 that is within less than 1 ppm of the calculated value for $C_{16}H_2S_7$. In the IR spectrum, the stretching mode for the α -C–H is found at 3105 cm^{-1} .

Pd-mediated reductive cyclization of *rac-4* gives crude reaction mixtures containing quasi-[8]circulene 7, as indicated by the singlet at δ 7.95 ppm in the ^1H NMR spectra and by the molecular ion (M^+) at m/z 417.8197 in the FABMS; however, the aromatic region of the ^1H NMR spectra also shows doublets, which are tentatively assigned to other debrominated byproduct (Figures S22 and S23, SI). Quasi-[8]circulene 7 is isolated in 70% yield (Figure S24, SI). Bis[7]helicene products, corresponding to intermolecular homocoupling of [7]helicene 4, are not detected.

Diheptyl Quasi-[8]Circulene 8. Vacuum pyrolysis of dibromo[7]helicene *rac-5* at 180 – 250°C provides quasi-[8]circulene 8, with optimum conditions at 250°C and recycling

(27) The mass loss near and above a temperature of 200°C is consistent with the onset of decomposition of [7]helicene *rac-4* observed as a color change in the melting point apparatus (ref 13).

SCHEME 3. Diheptyl Quasi-[8]Circulene 8



of the deposited *rac*-5 (Scheme 3). ^1H NMR spectra of the crude reaction mixtures show **8** as the major product, with negligible content of *rac*-5 (Figures S25 and S26, SI).

Pyrolysis of dibromo[7]helicene (+)-5 was also monitored by DSC, for which the sample is encapsulated inside a crimped aluminum pan, the most widely used standard sample preparation. Dibromo[7]helicene (+)-5 shows melting behavior (endothermic peak) with the onset temperature of 138 ± 2 °C, as reported previously.¹⁴ To explore pyrolysis of (+)-5, we increased the upper temperature limit of the DSC scan to 180 °C, and after the experiment we collected the sample for ^1H NMR analysis. The ^1H NMR spectrum of the DSC samples shows the presence of [7]helicene (+)-5 (δ 7.107) and a very small admixture of quasi-[8]circulene **8** (δ 7.989) (Figure S7, SI).^{28,29} Further extension of the upper temperature limit to 200 °C reveals an additional exothermic peak at about 182 °C (onset at 181 °C); after 1 min at 200 °C, the return scan is flat without significant changes in the heat flow (Figure 4).

^1H NMR and FABMS analyses of the recovered DSC samples indicate clean formation of quasi-[8]circulene **8**, with a melting point at 320–322 °C that is significantly above 200 °C (Figures S8 and S9, SI). Therefore, the exothermic peak at about 182 °C is assigned to a cyclization reaction in which dibromo[7]helicene (+)-5 is debrominated to produce quasi-[8]circulene **8**.

When simultaneous TG/DSC is carried out in a ceramic open sample pan, only the peak for melting of (+)-5 has a significant intensity in the DSC plot. In contrast to *rac*-4, the TG plot for (+)-5 shows only one process with a mass decrease corresponding to the loss of 1 equiv of Br_2 at about 330 °C (Figure S10, SI). The ^1H NMR spectrum of the recovered TG/DSC sample indicates formation of quasi-[8]circulene **8** (Figure S11, SI).

The tributyltin hydride-mediated cyclization of (+)-5 provides quasi-[8]circulene **8** at much milder conditions compared to those for pyrolysis. Analyses of the aromatic region of the ^1H NMR spectra for crude reaction mixtures indicate complete conversion of (+)-5 to quasi-[8]circulene **8**. Diheptyl quasi-[8]circulene **8** is readily isolated as a pale yellow solid by washing with organic solvents. Pd-mediated C–C bond forming reactions provide reaction mixtures containing **8** (NMR yield of 10%) and unreacted *rac*-5; no

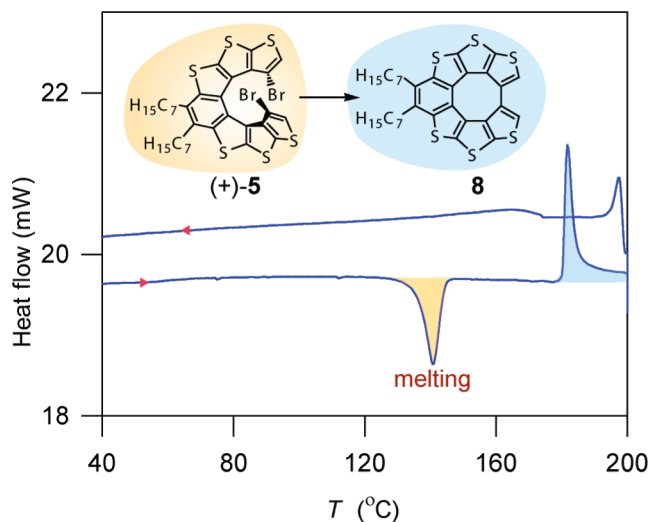
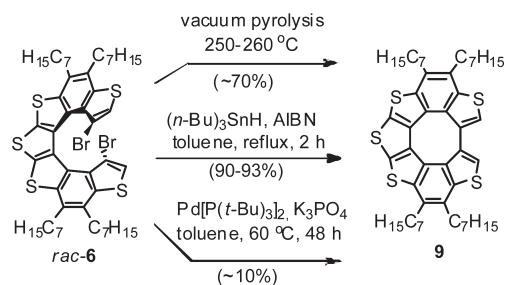


FIGURE 4. Differential scanning calorimetry for [7]helicene (+)-5. Scan rate 20 deg/min.

SCHEME 4. Tetraheptyl Quasi-[8]Circulene 9



evidence for products corresponding to intermolecular homocoupling of [7]helicene **5** is found.³⁰

Tetraheptyl Quasi-[8]Circulene 9. Following the same procedure for pyrolysis of dibromo[7]helicenes *rac*-5 and (+)-5, pyrolysis of dibromo[7]helicene *rac*-6 at 250–260 °C provides the corresponding quasi-[8]circulene **9** as a pale yellow solid in 70% isolated yields (Scheme 4).³¹

Simultaneous TG/DSC of *rac*-6 gives similar results to that for (+)-5. In particular, TG indicates a single process with a mass decrease corresponding to the loss of 1 equiv of Br_2 at about 330 °C, which is the same temperature as observed for (+)-5. The corresponding DSC plot shows the expected melting behavior (endothermic peak) at about 100 °C, and more importantly, another broad, exothermic peak at about 330 °C, which coincides with the loss of Br_2 observed in the TG plot (Figure 5).^{32,33}

Tributyltin hydride-mediated cyclization of *rac*-6 gives quasi-[8]circulene **9** in excellent (~90%) isolated yields. In contrast, Pd-mediated C–C bond forming reactions of dibromo[7]helicene *rac*-6 (and (+)-6) give complex reaction

(28) Vacuum pyrolysis of dibromo[7]helicene *rac*-5 at 180 °C leads to a low conversion to diheptyl quasi-[8]circulene **8** (Table S8, SI).

(29) In FABMS of dibromo[7]helicenes **4** and **5**, and bis(trimethylsilyl)-substituted derivatives of **4**–**6**, the $[\text{M} - 2\text{Br}]^+$ fragment ions have low relative amplitude (15% or less) compared to that of the $[\text{M}]^+$ or $[\text{M} + 2]^+$ ions; however, for dibromo[7]helicene **6**, the $[\text{M} - 2\text{Br}]^+$ fragment ion is dominant (Table S4 and Figure S15, SI).

(30) Bis(trimethylsilyl)-substituted quasi-[8]circulene **8**, designated as **8**-(TMS)₂, is also isolated in low yield from the McMurry reaction of the corresponding dibromo[7]helicene (SI).

(31) Quasi-[8]circulene **9** was isolated in low yields from acid-mediated deprotections of bis(trimethylsilyl)-substituted derivatives of [7]helicene *rac*-6 (ref 15).

(32) TG/DSC of *rac*-6, contained in a ceramic open sample pan that was covered with aluminum foil, is qualitatively similar to that in Figure 5. However, in TG, the loss of Br_2 is observed at a much lower temperature of about 265 °C and in the narrower temperature range; in DSC, the exothermic peak at about 265 °C is narrower and more intense (Figure S13, SI).

(33) ^1H NMR spectrum of the recovered TG/DSC sample indicates formation of quasi-[8]circulene **9** (Figure S14, SI).

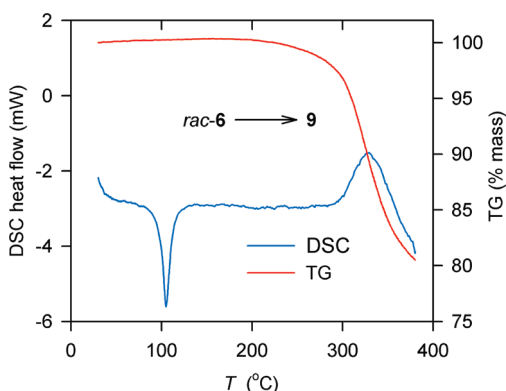


FIGURE 5. Simultaneous thermogravimetry and differential scanning calorimetry for [7]helicene *rac*-6. Scan rate 20 deg/min.

mixtures, as indicated by ^1H NMR (chloroform-*d*) spectra; quasi-[8]circulene **9** is isolated in $\sim 10\%$ yield. The major product is isolated in $\sim 50\%$ yield. In the mass spectrum (FAB) of this product, the peak with dominant intensity in the m/z 200–2000 range has an exact mass of 798.3442, which is within 1.6 ppm of the calculated value for $\text{C}_{48}\text{H}_{62}\text{S}_5$. Although this molecular formula is identical to that of quasi-[8]circulene **9**, ^1H and ^{13}C NMR spectra are consistent with the C_1 point group, thus indicating that this product is an isomer of **9**. Attempts to identify this product by X-ray crystallography were not successful.³⁴

Crystal Structure of Tetraheptyl Quasi-[8]Circulene 9. The X-ray structure of **9** was determined by synchrotron radiation, using a small colorless plate-shaped crystal (Figure 6).

The π -system of **9** adopts an approximately planar conformation as indicated by a small value (0.0650 Å) of mean deviation from a calculated least-squares plane including all benzene and thiophene rings (S1–S5, C1–C20). In the bay area, the C1–C2–C19–C20 torsion angle of $8.7(15)^\circ$ suggests a small out-of-plane distortion.

The π -systems of **9** slip-stack with the distance between least-squares planes of about 3.52 Å, forming columns along the crystallographic *a*-axis. Short intermolecular S...S contacts are observed within the columns and between neighboring columns varying between 3.53 and 3.64 Å (Figure 7).

Experimental and Calculated UV–Vis Absorption Spectra for Quasi-[8]Circulenes and [8]Circulenes. UV–vis absorption spectra for quasi-[8]circulenes **7–9** (Figure 8) show similar spectral patterns and are slightly blue-shifted compared to the corresponding [7]helicenes **4–6**.¹⁵ The spectra are progressively more red-shifted from **7** to **8** to **9** (Table S2, SI), which is similar to the trend found in the corresponding [7]helicenes.¹⁵ This result corroborates the increased electron delocalization from **7** to **8** to **9**, due to replacement of cross-conjugated thiophene rings in **7** with conjugated benzene rings.

Computational modeling is carried out to investigate whether the lack of atom linkage in quasi-[8]circulenes **7–9** would significantly affect the conformation and electronic structure, compared to those for the corresponding [8]circulenes. Quasi-[8]circulene **7** and [8]circulene (C_2S)₈, as well as simplified structures corresponding to **8** and **9**, in which the heptyl chains are replaced with methyl groups (Chart 1), are studied.

(34) One of the reviewers suggested the possibility of cyclization between the α - and β -positions of thiophenes.

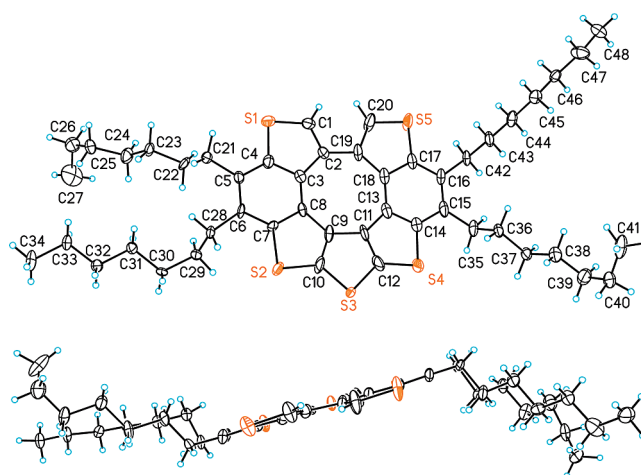
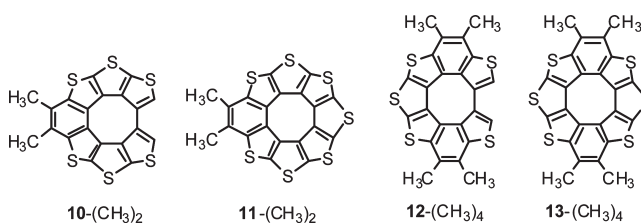


FIGURE 6. Molecular structure of tetraheptyl quasi-[8]circulene **9**. Carbon and sulfur atoms are depicted with thermal ellipsoids set at the 50% probability level. Disorder in two heptyl groups and in S3/S3d (60:40) are omitted for clarity. Disorder is illustrated in Figure S1, SI.

CHART 1. Structures of Simplified Quasi-[8]Circulenes and [8]Circulenes



Conformations for **7**, (C_2S)₈, **10**-(CH₃)₂, **11**-(CH₃)₂, **12**-(CH₃)₄, and **13**-(CH₃)₄ are assessed by full geometry optimizations and vibrational frequency calculations within the respective point groups of symmetry, using the B3LYP/6-31G(d,p) method (Table S13, SI).³⁵ We found that all of the three [8]circulenes, (C_2S)₈, **11**-(CH₃)₂, and **13**-(CH₃)₄, possess planar π -systems.³⁶ For quasi-[8]circulenes, the planar geometries are either shallow minima with very small, positive vibrational frequency (6 cm^{-1} for **7**) or structures with one imaginary frequency ($i21\text{ cm}^{-1}$ for **10**-(CH₃)₂ and $i101\text{ cm}^{-1}$ for **12**-(CH₃)₄). These very small, positive vibrational frequencies and imaginary frequencies correspond to the out-of-plane distortion of the π -system with the disrotatory movement of the CH bonds in the bay area of quasi-[8]circulene. The corresponding nonplanar geometries for **10**-(CH₃)₂ and **12**-(CH₃)₄ with the C_2 point groups of symmetry are minima; however, their energy is practically identical and only 4.7 kcal mol⁻¹ lower than the planar C_{2v} -symmetric structures, respectively.³⁷ For C_2 -symmetric quasi-[8]circulenes **10**-(CH₃)₂ and **12**-(CH₃)₄, the C(H)–C–C–

(35) Frisch, M. J.; et al. *Gaussian 03*, Revision E.01; Gaussian, Wallingford, CT, 2004.

(36) This result is in agreement with the previously reported X-ray structure and calculations for [8]circulene (C_2S)₈; ref 6.

(37) (a) For quasi-[8]circulene **10**-(CH₃)₂, the C_2 -symmetric minimum and the C_{2v} -symmetric transition state possess similar energies; the C_2 -symmetric structure is lower in energy by 0.04 kcal mol⁻¹, but after zero-point vibrational energy (ZPVE) correction, the C_{2v} -symmetric structure is lower in energy by 0.04 kcal mol⁻¹. (b) For quasi-[8]circulene **12**-(CH₃)₄, the C_2 -symmetric minimum is lower in energy by 5.00 kcal mol⁻¹ before ZPVE correction and by 4.69 kcal mol⁻¹ after ZPVE, compared to that of the C_{2v} -symmetric transition state.

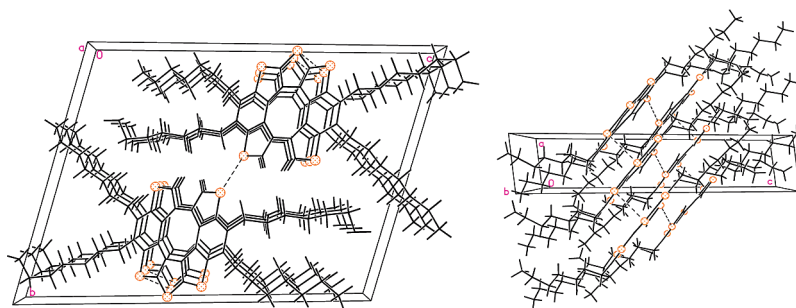


FIGURE 7. Crystal packing plots of tetraheptyl quasi-[8]circulene **9**. Left plot: View along the *a*-axis. Right plot: View along the *b*-axis. Sulfur atoms and short S...S contacts are indicated with yellow-orange circles and dashed lines, respectively.

C(H) torsion angles, analogous to the C1–C2–C19–C20 torsion angle of $8.7(15)^\circ$ in the X-ray structure of **9**, are 7.8° and 28.6° , respectively. These results suggest that the preference for nonplanar geometry of the π -system is increasing, with the greater number of benzene rings, but overall the potential energy surfaces for all three quasi-[8]circulenes are rather shallow with nearly planar geometries.³⁸

The UV–vis absorption spectra for **7**, $(C_2S)_8$, **10**-(CH₃)₂, **11**-(CH₃)₂, **12**-(CH₃)₄, and **13**-(CH₃)₄ are calculated by using the TD-B3LYP/6-31G(d,p) method with the IEF-PCM-UAHF solvent model for cyclohexane.³⁵ The calculated spectra for quasi-[8]circulenes **7**, **10**-(CH₃)₂, and **12**-(CH₃)₄ show an excellent agreement with experimental spectra for the corresponding quasi-[8]circulenes **7**, **8**, and **9**; in particular, the UV–vis spectra are progressively more red-shifted with the increasing number of benzene rings (Figure 8). Most importantly, the calculated spectra of [8]circulenes and the corresponding quasi-[8]circulenes possess similar spectral patterns. Overlapping onsets of absorption are observed, with the exception of quasi-[8]circulene **7** and the corresponding *D*_{8h}-symmetric [8]circulene $(C_2S)_8$, in which the lowest energy transitions are symmetry-forbidden.³⁹ Thus, we conclude that both conformations and electronic structures for the studied quasi-[8]circulenes are similar to those for the corresponding [8]circulenes.

Effect of Helix Structure on the Intramolecular Cyclization Reaction of [7]Helicenes to Quasi-[8]Circulenes. The helix structure dictates the geometry at the two C–Br termini of the inner helix in [7]helicene (Table S1, SI), and therefore it may affect the cyclization reaction forming the C–C bond between the termini carbons.

We postulate that shorter C...C distances between the termini of the inner helix in [7]helicenes facilitate cyclization by pyrolysis, i.e., [7]helicene **6**, with the shortest C...C distance of 3.30 Å, is most efficiently converted to the corresponding quasi-[8]circulene. Notably, tributyltin hydride-mediated radical cyclization of **4**–**6**, which is carried out in solution under relatively milder conditions, appears to be practically insensitive to the C...C distances, and thus provides a general method for the synthesis of quasi-[8]circulenes from dibromo[7]helicenes.

Pd-mediated reductive cyclization to quasi-[8]circulene is most efficient for [7]helicene **4**. This result may be rationalized by considering the palladium complex prior to the

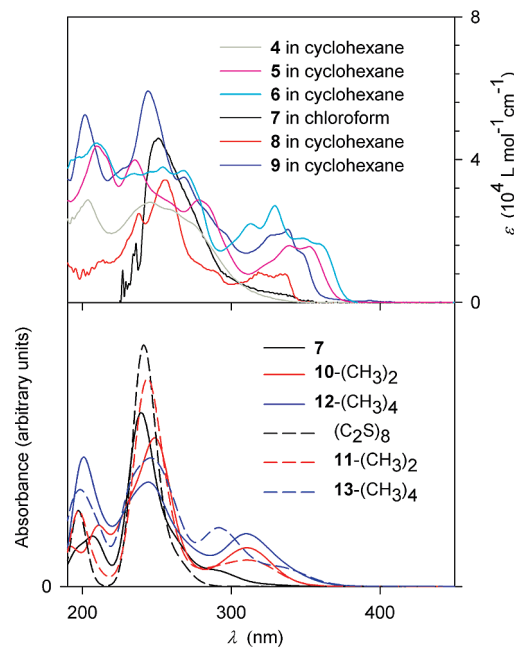


FIGURE 8. UV–vis absorption spectra. Top plots: Experimental spectra for quasi-[8]circulenes **7**–**9**. Bottom plots: Calculated spectra for quasi-[8]circulenes **7** (C_{2v}), **10**-(CH₃)₂ (C_2), and **12**-(CH₃)₄ (C_2) (solid lines), and the corresponding [8]circulenes $(C_2S)_8$, **11**-(CH₃)₂, and **13**-(CH₃)₄ (dashed lines). All spectra are calculated at the TD-B3LYP/6-31G(d,p) level with the IEF-PCM-UAHF solvent model for cyclohexane; the ground state geometries are optimized at the B3LYP/6-31G(d,p) level in the gas phase. Because of low solubility of **7** and **8** in cyclohexane, their experimental spectra are only qualitative.

reductive elimination.^{40,41} Formation of such a complex would require distortion of the helix so both termini are oriented in the same direction to accommodate the C–Pd–C bond angle of about 90° . This distortion of the helix, which may be analogous to that calculated for the C_s -symmetric transition state for racemization of a typical [*n*]helicene ($n < 9$),⁴² will be most facile when the termini are the least overlapping as in the helix of **4**.

Conclusion

Intramolecular cyclization at the two bromine-substituted termini of the inner helix in [7]helicene provides a pathway to

(38) Increasing preference for nonplanarity is expected as, already with seven annelated benzene rings, [7]circulene adopts saddle-shape geometry: ref 10a.

(39) Calculated onsets for the lowest energy electronic transitions (λ_{onset} in Table S13, SI) are similar, with small red shifts for quasi-[8]circulenes.

(40) Culkin, D. A.; Hartwig, J. F. *Organometallics* **2004**, *23*, 3398–3416.
(41) Altman, R. A.; Hyde, A. M.; Huang, X.; Buchwald, S. L. *J. Am. Chem. Soc.* **2008**, *130*, 9613–9620.

(42) Janke, R. H.; Haufe, G.; Würthwein, E.-U.; Borkent, J. H. *J. Am. Chem. Soc.* **1996**, *118*, 6031–6035.

a quasi-[8]circulene, a cyclic structure of the annelated aromatic rings that closely resembles [8]circulene. Tributyltin hydride-mediated radical cyclization gives quasi-[8]circulenes in excellent yields, and this cyclization reaction is practically insensitive to the geometry of the termini of inner helix in [7]helicenes. We found that the lack of atom linkage in thiophene-rich quasi-[8]circulenes does not significantly affect conformation and electronic structure, compared to those for the corresponding [8]circulenes.

Experimental Section

General Procedures for Cyclization of [7]Helicenes 4–6 to Quasi-[8]Circulenes 7–9: Vacuum Pyrolysis. [7]Helicene was pyrolyzed at 180–290 °C, with the vacuum ($p \gg 0.1$ mTorr) adjusted for each [7]helicene for optimum trade-off between rate of sublimation/evaporation and of quasi-[8]circulene formation. After several hours, the sublimed material (primarily unreacted [7]helicene) was recycled to the pyrolysis vessel with solvent, and the pyrolysis was resumed. This process was repeated until the starting [7]helicene was consumed. From pyrolysis of *rac*-4, quasi-[8]circulene 7 could not be isolated. From pyrolysis of 5 at ~250 °C, quasi-[8]circulene 8 could only be obtained as a brown solid and in low yield either from the residue at the bottom of the pyrolysis vessel or following rapid filtration through silica plug with benzene. From pyrolysis of 6 at 250–260 °C (65.0 mg, 0.0678 mmol), quasi-[8]circulene 9 (39.1 mg, 72%) was isolated as a pale yellow solid after column chromatography (silica, hexane). Residual impurities in the aliphatic region of the NMR spectra were removed by washing with methanol and pentane.

Tributyltin Hydride-Mediated Cyclization. A solution of *n*-Bu₃SnH (2–6 equiv) and AIBN (2–4 equiv) in toluene was added dropwise to a refluxed solution of [7]helicene (2–25 mg, 1 equiv) in toluene. The total volume of toluene corresponded to about 6 mM concentration of [7]helicene in the resulting reaction mixture. After 2–4 h under reflux, the toluene was removed under vacuum, to provide a crude product as a sticky solid. Sequential washing with methanol and acetone or methanol and pentane provided quasi-[8]circulene as a white solid (7) or pale yellow solid (8 and 9) in good yield (76–93%).

Pd-Mediated Cyclization. [7]Helicene (1.9–51 mg, 1 equiv), Pd[P(*t*-Bu)₃]₂ (1–2.5 equiv), and K₃PO₄ (2–7 equiv) in toluene (0.5–4.5 mL) were stirred at 60–80 °C for 20–48 h. The reaction mixture, starting from *rac*-4 (6.08 mg), was centrifuged, and then the insoluble part was treated with water, methanol, acetone, and ethyl acetate, to provide quasi-[8]circulene 7 as a brown solid (3.14 mg, 71%). The reaction mixture, starting from *rac*-5 (1.6 mg), was filtered through Celite, and then concentrated in vacuo to provide the crude product; the ¹H NMR spectrum and FABMS showed quasi-[8]circulene 8, starting material, and another byproduct. The reaction mixture, starting from *rac*-6 (34.6 mg), was concentrated and worked up with chloroform/water; the chloroform layer was filtered through Celite and concentrated to provide the crude product. Reactions

starting from (+)-6 provided similar crude products (Figure S35, Supporting Information). Chromatography (deactivated silica, ethyl acetate, chloroform, hexane), followed by treatments with solvents, gave quasi-[8]circulene 9 as a yellow solid (2.9 mg, 10%) and another product (15.7 mg, Supporting Information).

Quasi-[8]circulene 7: Mp > 400 °C (under vacuum). ¹H NMR (500 MHz, chloroform-*d*) δ 7.95 (s, 2 H). LR/HR FABMS (ONPOE) *m/z* (ion type, %RA for *m/z* 200–2000, deviation from formula) 417.8197 ([M]⁺, 100%, 1.2 ppm for ¹²C₁₆¹H₂³²S₇). LR/HR EIMS *m/z* (ion type, %RA for *m/z* 150–440, deviation for the formula) 417.8204 ([M]⁺, 100%, 0.6 ppm for ¹²C₁₆¹H₂³²S₇). IR (ZnSe, cm⁻¹) 3105 (α -C–H of thiophene), 2961, 2918, 2850 (C–H).

Quasi-[8]circulene 8: Mp 320–322 °C (under nitrogen). ¹H NMR (500 MHz, chloroform-*d*) δ 7.983 (s, 2 H), 3.062–3.029 (m, 4 H), 1.844–1.781 (m, 4 H), 1.556–1.489 (m, overlapped with H₂O, 4 H), 1.454–1.252 (m, 12 H), 0.912 (t, *J* = 7 Hz, 6 H). LR/HR FABMS (3-NBA) *m/z* (ion type, % RA for *m/z* 200–1500, deviation for the formula) 608.0839 ([M]⁺, 100%, -1.7 ppm for ¹²C₃₂¹H₃₂³²S₆). IR (ZnSe, cm⁻¹) 3111 (α -C–H of thiophene), 2956, 2923, 2853, 1467.

Quasi-[8]circulene 9: *R_f* 0.56 (hexane). Mp 197–199 °C (lit.¹⁵ mp 198–200 °C). ¹H NMR (500 MHz, chloroform-*d*) δ 7.894 (s, 2 H), 3.086–3.035 (m, 8 H), 1.846–1.770 (m, 8 H), 1.435–1.422 (m, 8 H), 1.253–1.101 (m, 16 H), 0.914–0.766 (m, 12 H). ¹³C NMR (125 MHz, chloroform-*d*) aromatic region, expected 10 resonances, found 10 resonances at δ 143.2, 140.2, 136.9, 135.06, 134.1, 131.0, 130.3, 127.9, 126.7, 125.4, aliphatic region, expected 14 resonances, found 11 resonances at δ 32.07, 32.05, 31.8, 30.20, 30.18, 29.96, 29.79, 29.70, 29.1, 22.7, 14.1. LR/HR FABMS (3-NBA) *m/z* (ion type, %RA for *m/z* 400–1200, deviation for the formula) 798.3448 ([M]⁺, 100%, 0.8 ppm for ¹²C₄₈¹H₆₂³²S₅). IR (ZnSe, cm⁻¹) 3136 (weak), 2956, 2920, 2853, 1471, 1107, 802.

Acknowledgment. This research was supported by the National Science Foundation (CHE-0414936 and CHE-0718117). ChemMatCARS Sector 15 is principally supported by the National Science Foundation/Department of Energy under Grant No. CHE-0087817. The Advanced Photon Source is supported by the U.S. Department of Energy, Basic Energy Sciences, Office of Science, under Contract No. W-31-109-Eng-38. We thank Dr. Rick Albro and Professor Craig Eckhardt for the help with the initial DSC measurements. We thank Ms. Carita Kordik for MS studies. We thank Dr. Kausik Das for growing single crystals of quasi-[8]circulene 9.

Supporting Information Available: Complete ref 35 and description of experimental detail and product characterization, including X-ray crystallographic file in CIF format. This material is available free of charge via the Internet at <http://pubs.acs.org>.